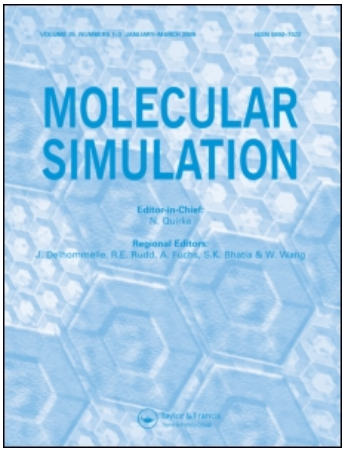

Molecular Simulation
Publication details, including instructions for authors and subscription information:
http://www.informaworld.com/smpp/title~content=t713644482

Microstructure of Water At the Level of Three-particle Correlation Functions As Predicted by Classical Intermolecular Models

Csaba Peltz[a]; András Baranyai[a]; Ariel A. Chialvo[bc]; Peter T. Cummings[bc]
[a] Department of Theoretical Chemistry, Eötvös University, Budapest 112, Hungary [b] Chemical Sciences Division, Oak Ridge National Laboratory, Oak Ridge, TN, USA [c] Department of Chemical Engineering, University of Tennessee, Knoxville, TN, USA

Online publication date: 26 October 2010

To cite this Article Peltz, Csaba , Baranyai, András , Chialvo, Ariel A. and Cummings, Peter T.(2003) 'Microstructure of Water At the Level of Three-particle Correlation Functions As Predicted by Classical Intermolecular Models', Molecular Simulation, 29: 1, 13 — 21
To link to this Article: DOI: 10.1080/0892702031000065692
URL: http://dx.doi.org/10.1080/0892702031000065692

Molecular Simulation, 2003 Vol. 29 (1), pp. 13–21

Microstructure of Water at the Level of Three-particle Correlation Functions as Predicted by Classical Intermolecular Models

CSABA PELTZ[a], ANDRÁS BARANYAI[a,*], ARIEL A. CHIALVO[b,c] and PETER T. CUMMINGS[b,c]

[a]*Department of Theoretical Chemistry, Eötvös University, 1518 Budapest 112, PO Box 32, Hungary;* [b]*Chemical Sciences Division, Oak Ridge National Laboratory, Oak Ridge, TN 37831-6110, USA;* [c]*Department of Chemical Engineering, University of Tennessee, 419 Dougherty Engineering Building, Knoxville, TN 37996-2200, USA*

We compared the microscopic structure of liquid water at ambient conditions predicted by six classical intermolecular potential models. Applying their accepted acronyms were the SPC (Simple Point Charge), SPC/E (SPC extended), MSPC/E (SPC/E modified), TIP4P (Transferable Intermolecular Potential, four point charges), TIP5P (TIP, five point charges), and the PPC (Polarizable Point Charge) intermolecular potential models. Configurations of computer simulations were used to study the structure at the level of partial three-particle correlation functions. We created contour maps for visual evaluation, calculated overlap integrals of the three-particle correlation functions of the models to quantify their similarity, and determined their distance-dependent three-particle entropy contribution. The SPC/E and the TIP4P water models generate quite similar structures, while the SPC and the MSPC/E pair exhibit the largest discrepancies. The structure of the PPC is the most ordered and the SPC structure is the most disordered among the studied interaction models.

Keywords: Three-particle correlation; Classical intermolecular models; SPC; TIP4P

INTRODUCTION

There is an ongoing effort to predict and explain the macroscopic properties of water on the basis of its microscopic structure. Results of X-ray and neutron diffraction experiments have been known for decades [1–3] (even though there is still an ongoing discussion on how to assess their accuracy) [4] and the number of papers reporting calculations and simulations based on some molecular models is enormous [5,6]. The use of classical approaches to model water is motivated by the possibility of almost limitless quasi-experimental investigation of water through molecular simulation. In addition to the static structure, dielectric and transport properties, bulk and interfacial behavior, as well as phase equilibrium can be studied by these methods. Classical computational modeling is still competitive with *ab initio* simulations, since the need of massive computational resources limits the system size and the time range studied by *ab initio* molecular dynamics [7–9]. Inherent limitations of diffraction experiments also require input from successful classical models [10]. Considering liquid water as a 2:1 mixture of hydrogen and oxygen, three different partial structure functions or correlation functions are needed to describe the microscopic structure at the level of site–site pair-correlation functions. Recently, Sorenson *et al.* [11,12] carried out a X-ray scattering experiment on pure water at ambient temperature and pressure. After a careful processing of their data, they carried out an extensive comparison of the oxygen–oxygen partial correlation functions taken from a variety of measurements and simulation studies. Based on their experimentally determined $g_{OO}(r)$, they qualified several classical potential models and results of *ab initio* simulations.

Obviously, the fine structure of water is manifested only in the complete hierarchy of many-body correlation functions. An important feature of it is

*Corresponding author.

ISSN 0892-7022 print/ISSN 1029-0435 online © 2003 Taylor & Francis Ltd
DOI: 10.1080/0892702031000065692

the hydrogen-bond network that has also been extensively studied [13–15]. A typical statistical mechanical approach to the study of molecular liquids is to expand the pair-correlation function of molecules in terms of spherical harmonics. This analysis was done by Soper [16] who used experimental data for that purpose. Local density distributions have been calculated by Svishchev and Zassetsky [17] by molecular dynamics simulations determining the distinct part(s) of the van Hove function. In addition to these more recent studies, there are numerous papers in the literature where attempts have been made to describe the structure of liquid water beyond the level of pair correlations [17,18].

An important product of the above mentioned studies is the critical evaluation and comparison of existing classical water models. This assessment, in turn, can lead to models being better representations of reality, and eventually, to a deeper understanding of the properties of water. The purpose of the present paper is to provide additional information about some frequently used classical models of water. We use the complete set of partial three-body correlation functions for this purpose in the site–site formalism. Since extra information in higher order correlation functions is important from medium density, we expect to find discrepancies in the predicted water structure that might be unnoticeable at the level of pair correlations. Note, however, that our primary goal is not to assess the realism with which current water models describe the behavior of water, but rather to search for additional structural information (here, at the level of triple correlation functions) that could be used to uniquely discriminate among models.

The paper is organized as follows. In the second section, we briefly describe the six water intermolecular potentials used in this investigation. In the third section, we describe how the configurations generated by molecular dynamics applying these models are used to create the maps of the three-particle correlation functions when water is considered as the 2:1 hydrogen–oxygen mixture. In the fourth and fifth sections, we give a quantitative measure of the structural similarity among different models in terms of both the overlap integrals and the distance dependence of the three-particle entropy contributions. Finally, in the sixth section, we conclude the study.

TABLE I Thermophysical properties of water at ambient conditions: configurational internal energy U_c and enthalpy of vaporization ΔH_{vap} in kcal/mol, specific heat at constant pressure C_p in kcal/(mol K), isothermal compressibility $10^6\,\kappa$ in atm, dielectric constant ε and diffusion coefficient D in $10^5\,\text{cm}^2/\text{s}$

Model	U_c	ΔH_{vap}	C_p	$10^6\,\kappa$	ε	D
SPC	−9.89	10.77	23.4	27	63 ± 31	4.3
SPC/E	−9.80	–	–	–	81.3	2.4
MSPC/E	−10.38	10.94	–	–	–	–
TIP4P	−9.79	10.66	19.3	35	29 ± 13	–
TIP5P	−9.87	10.46	29.1	41	81 ± 2	2.6
PPC	−9.85	10.96	22.2	63	78.3	2.9
Expt.	−9.92	10.51	18.0	45.8	77.7	2.3

INTERMOLECULAR POTENTIAL MODELS FOR WATER

Perhaps the simplest and most frequently used models for water are described by a planar rigid geometry and simple point charges (SPCs), i.e. resulting in non-polarizable models. In addition, to account for the large polarization effects over the ideal gas water dipole moment of $1.85D$, these models involve augmented electrostatic charges that give rise to permanent dipole moments $1.85D < \mu < 2.4D$ [6]. The so-called SPC water model [19] is considered to be the first three-site water model that gave a realistic representation of water at ambient conditions (Table I). This model is described as a Lennard–Jones potential and corresponding electrostatic charges for the O–O interactions plus two embedded electrostatic charges at 1Ĺ from the oxygen, forming a tetrahedral HOH angle of 109.47° (see Table II for force field information), i.e.

$$\phi_{\text{SPC}}(r_{12},\omega_1,\omega_2) = \sum_{\alpha,\beta=1}^{3} \frac{q_1^\alpha q_2^\beta}{r_{12}^{\alpha\beta}} + 4\varepsilon_{\text{OO}}\left[\left(\frac{\sigma_{\text{OO}}}{r_{\text{OO}}}\right)^{12} - \left(\frac{\sigma_{\text{OO}}}{r_{\text{OO}}}\right)^{6}\right] \quad (1)$$

TABLE II Potential parameters of rigid water models

Model	σ_{OO} (Ĺ)	ε_{OO}/k_B (K)	$q_H \equiv -q_O/2$	*Sites*	*R_OH (Å)*	$\mu(D)$
SPC	3.166	78.23	0.4100	3	1.0	2.27
SPC/E	3.166	78.23	0.4238	3	1.0	2.35
MSPC/E	3.116	74.70	0.4108	3	0.9839	2.24
TIP4P	3.153	78.08	0.5200	4	0.9572	2.18
TIP5P	3.120	80.6	0.2410*	5	0.9572	2.19
PPC	3.234	72.07	0.486†	4	0.943	2.14†

* $q_H = -q_L$. † These values correspond to the zero field or permanent charge/dipole.

where the subscript OO represents oxygen–oxygen interactions, q_i^α is the charge on site α on molecule i, $r_{12}^{\alpha\beta}$ is the distance between site α on molecule 1 and site β on molecule 2, ε and σ are the Lennard–Jones' energy and size parameters, respectively. The SPC model was among the first for which the vapor–liquid phase envelope was determined by GEMC [20]. The result is an estimate of the model's critical point, $T_c \approx 587\,\mathrm{K}$ and $\rho_c \approx 0.27\,\mathrm{g/cm^3}$, in comparison to the actual values [13] of $T_c = 647\,\mathrm{K}$ and $\rho_c = 0.32\,\mathrm{g/cm^3}$.

There are several variations around this model, including the SPC/E (SPC extended) [21] and its later modification MSPC/E (SPC/E modified) [22]. These modifications are simply re-parameterizations of either the charges, due to a missing polarization term in the original SPC Hamiltonian, i.e. $E_p = (2\alpha)^{-1}(\mu - \mu_{\mathrm{gas}})^2$ in the case of the SPC/E, or both charges and Lennard–Jones parameters for the case of the MSPC/E. In both cases, the re-parameterization, based on matching the experimental pressure/density and internal energy of the water at ambient conditions, translate into different vapor–liquid equilibrium as well as structural and dielectric behavior [22]. The vapor–liquid phase envelope of SPC/E was determined through an indirect molecular dynamics approach [23] resulting in a better agreement with the phase diagram of real water in that the critical point of the SPC/E model is $T_c \approx 651\,\mathrm{K}$ and $\rho_c \approx 0.326\,\mathrm{g/cm^3}$.

While the MSPC/E model improves the representation of the phase envelope over that of the SPC model, the SPC/E representation is still the best among all non-polarizable water models. However, the MSPC/E model gives a better prediction of the vapor pressure, and partial improvements on the enthalpy of vaporization (at low temperature) and second virial coefficients (at high temperature). The predicted critical conditions for this model are $T_c \approx 602\,\mathrm{K}$ and $\rho_c \approx 0.31\,\mathrm{g/cm^3}$.

The TIP4P (Transferable Intermolecular Potential, four point charges) water model is a four-site rigid model (three Coulombic sites and a Lennard–Jones site) [24] where the negative charge is located in the bisectrix of the HOH bond angle and 0.15 Å away from the Lennard–Jones oxygen site. The HOH bond angle is 104.52°, and the OH bond length is 0.9572 Å. The TIP5P (TIP, five point charges) water model, recently developed by Mahoney and Jorgensen [25], involves a five-site non-planar rigid geometry (see Fig. 1 of Ref. [25]). The oxygen and hydrogen sites are located in a plane, following the TIP4P geometry. The remaining two sites, bearing the same negative charge $q_L = -q_H$, are located on a plane perpendicular to that defined by the HOH angle with an LO bond length of 0.7 Å (distance from the lone negative charge L to the oxygen site), with a tetrahedral LOL bond angle (109.47°). Consequently, this pair-potential involves an oxygen–oxygen Lennard–Jones interaction plus four Coulombic interactions (from two hydrogen sites and two L sites).

The polarizable point charge (PPC) model of Kusalik *et al.* [26] retains the simplicity of most non-polarizable three-site models while incorporating the nonadditive polarization through PPCs that fluctuate in response to the local electric field. The novelty in this model is that the electric-field dependence of the point charges has been determined by quantum-chemical calculations using a commercial package. According to the latest work of Svishchev *et al.* [27], this model predicts the following critical conditions: $T_c \approx 606\,\mathrm{K}$ and $\rho_c \approx 0.30\,\mathrm{g/cm^3}$.

COMPARISON OF CONTOUR MAPS OF THE MODELS

All simulations were performed at isothermal–isochoric conditions with a total of 256 water molecules at the temperature of $T = 298\,\mathrm{K}$, for the density $\rho = 1.0\,\mathrm{g/cm^3}$ using a Nosé thermostat [28]. The Newton–Euler equations of motion were integrated using a 5th order and 4th order Gears' predictor–corrector [29] for the translational and rotational degrees of freedom, respectively, with a time step of 1.0 fs. The rigid-body orientations were described by the quaternion formalism [30]. Long-ranged electrostatic interactions were handled by a molecular reaction field approach [31], and the non-electrostatic interactions were truncated at a distance $r_c = 3.0\sigma_{\mathrm{OO}}$, using the standard long-range pressure and configurational internal energy corrections. After an equilibration period of 100 ps, 2000 system configurations were dumped to a file every 0.1 ps to perform the correlation function analysis.

Using the configuration snapshots we determined partial three-particle correlation functions. For this purpose we generalized the method of Baranyai and Evans for a multi-component system [32–35]. This way we obtained six different correlation functions: g_{HHH}, g_{HHO}, g_{HOO}, g_{OHH}, g_{OHO}, and g_{OOO}. Since their normalization is different, the atom type considered as a center cannot be permuted in the mixed cases. The $g(r, s, t)$ functions were calculated with the limits of $r, s \le L/4$ and $t \le L/2$, where L is the length of the simulation box. Hence, the results presented in the following are quite local, valid only within the limits given above.

Using these functions we created contour maps. By keeping one distance fixed and varying the other two, the curves indicate points with identical value of the function. Typical maps are shown in Fig. 1. These functions are contour maps of g_{OOO} which should be symmetrical by permuting its variables.

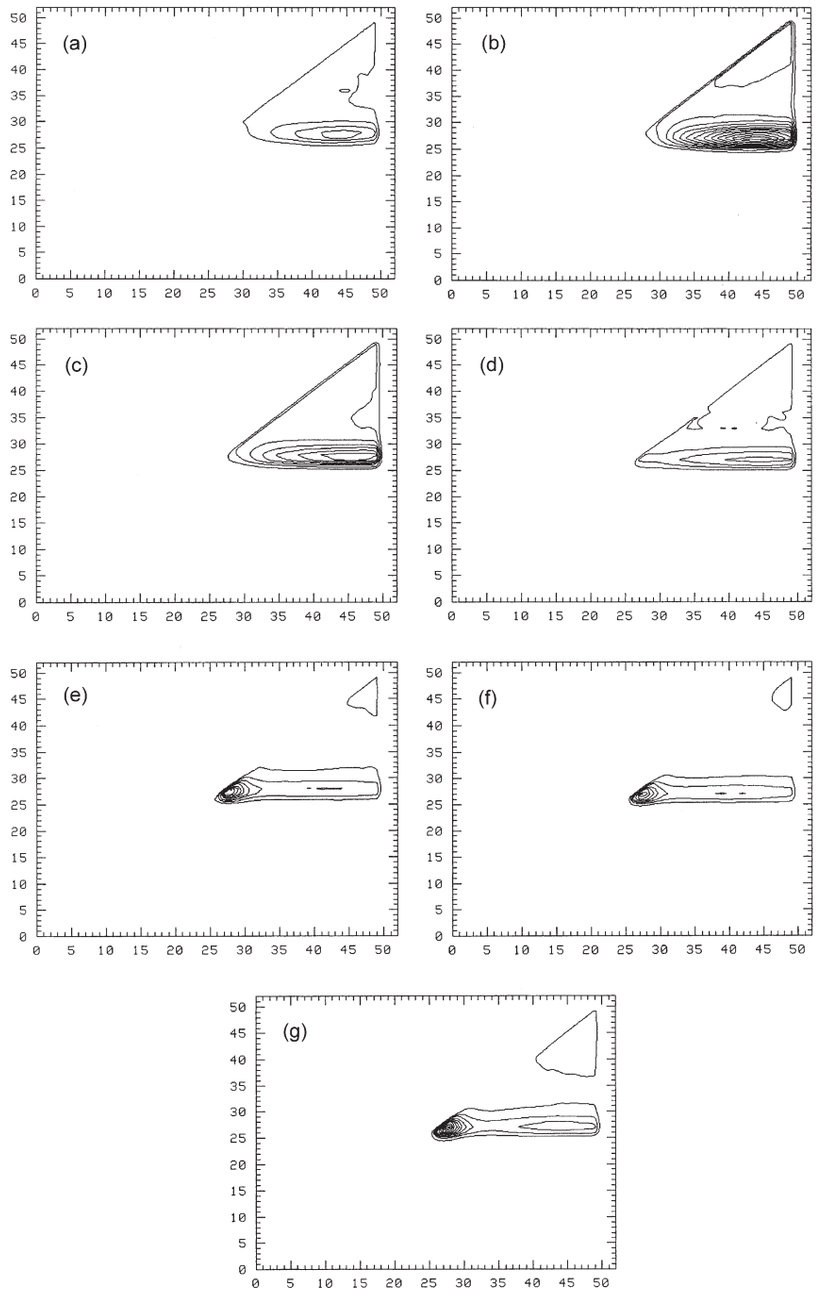

FIGURE 1 The contour maps show g_{OOO} distribution sections of the SPC and the MSPC/E models at ambient conditions. We omitted the mirror image of the maps above the $x = y$ line. The width of a bin is 0.0988 Å. The appearance of an additional curve marks an increase of the height by 1. The corresponding peaks of the two models are presented in the same row with the exception of the third SPC map which for obvious reasons is compared to two MSPC/E maps. In the following the number in front of and after the acronym of the model marks the row of Table III and the fixed third bin, respectively. (a) 2nd SPC; 26th. (b) 2nd MSPC/E; 27th. (c) 3rd SPC; 29th.(d) 3rd MSPC/E; 30th. (e) 5th SPC; 41st. (f) 5th MSPC/E; 37th. (g) 6th MSPC/E; 44th.

However, in the figures we adopted the convention that $r \geq s$, i.e. the horizontal variable is always larger than the vertical one. So, the other half of the figure can be obtained by creating the mirror image of the map over the $r = s$ line. Increasing of the height of the function by 1 generates an additional contour curve; thus, counting the number of curves around a peak gives a good estimate of its height.

The g_{OOO} and the g_{HHH} functions present a sort of a skeleton of the structure. In this respect g_{OOO} is the only partial which is independent from the preset intra-molecular structure of the model. First, we studied visually the g_{OOO} and g_{HHH} maps, to see both qualitative and quantitative differences between the arrangements created by the different models. The discrepancies were more pronounced in

TABLE III The first seven peaks of the g_{OOO} function

	Models					
Peaks	*SPC*	*SPC/E*	*MSPC/E*	*PPC*	*TIP4P*	*TIP5P*
1	–	28,43,25	28,45,25*	28,42–43,25	28,42,25	28,43,25
	–	0.85	2.0	0.43	0.69	1.67
2	28,44,26	–	28,44,27	–	–	–
	4.4	–	11.0	–	–	–
3	28,45,29	28,44–45,29	28,44,30	28,44,29	28,44,29	–
	7.6	3.6	3.6	9.3	8.3	–
4	28,29,32	28,28,33	28,28,32	28,28,33	28,28,33	28,28,34
	3.7	4.6	3.7	4.7	4.5	4.1
5	28,28,41	28,28,38	27,27,37	28,28,37	28,28,38	28,28,38
	8.7	8.3	8.8	8.8	8.8	6.8
6	–	28,28,44*	27,27,44	28,28,44*	28,28,45*	28,28,43*
	–	11.6	13.9	0.002	11.9	9.5
7	28,28,49–	–	–	–	–	28,28,49–

The three numbers represent the (r, s, t) bins with a local maximum. The height of the peaks in numbers is given below. These local maxima were identified visually. The third number (t) is the one kept fixed.

the former case, therefore, we collected the first seven local maxima of the g_{OOO} function. A summary of them is given in Table III. The maximum is identified by the three indices (r, s, t) of its bin. The width of a bin is 0.0988 Å. The last index (t) is the one fixed. Sometimes, the maximum was practically the same for several maps (several consecutive values of the last index with identical first and second indices), therefore in these cases we chose the bin in the middle and marked the third index (t) with a star.

The maxima for different interaction models are grouped in the same row in Table III if their three indices are identical or very close to one another. If we study Table III carefully we can notice that only three qualitatively different triplet structures were found. Rows 1, 2, 3, 6 and 7 all mark triplets resembling the structure of hexagonal ice. Two distances are within the range of 2.7–3.0 Å, while the third one represents the hypotenuse of the triangle with a tetrahedral facing angle. Rows 4 and 5, however, are different. They do not match into the structure of hexagonal ice. Expectedly, they show that the structure of liquid water is considerably distorted compared to that of hexagonal ice. The smaller angles of these triangles are responsible for the smaller density of liquid water.

By studying Table III we can see that the first column (SPC model) differs the most from the rest. In the light of these data and further properties of the maps not presented in Table III, the largest discrepancies can be seen between the SPC and the MSPC/E models. Therefore, to give some visual indication of it, in Fig. 1, we present the maps of some peaks shown in Table III of the SPC and the MSPC/E water models.

The mixed correlation functions possess inherent differences as a result of the design of the water molecule that makes their purely configurational comparison less meaningful and numerically uncomfortable (i.e. the intra-terms require special care). An important exception is the g_{OHO} function that contains information about hydrogen bonding. The most convenient map of this function can be obtained if the fixed variable (t) is the internal O–H distance of the particular model. Then the abscissa (r) corresponds to the O–O, and the ordinate (s) corresponds to the external O–H distances. In Fig. 2, we show these maps for the six different models. The most striking feature of these curves is that, in addition to the elliptically shaped high peak marking the presence of strong hydrogen bonding, the SPC and SPC/E models have a much lower but not negligible, extended peak at larger distances. The presence of this feature is much less significant in the other structures.

OVERLAP INTEGRALS AS QUANTITATIVE MEASURES OF SIMILARITY

It might be useful to give a quantitative measure of the structural similarity of water generated by different interaction models. We introduced two normalized factors for this purpose. If f and g are two real functions defined on the same set of variables then the quantity O with values between 0 and 1 will characterize the similarity of these two functions:

$$O = \frac{\int fg}{\int f \cdot \int g} \tag{2}$$

An alternative method for the same purpose is given as follows:

$$O' = \frac{\int \min(f, g)}{\min(\int f, \int g)} \tag{3}$$

As a result of model differences it is pointless to calculate these integrals for the mixed partials. Thus,

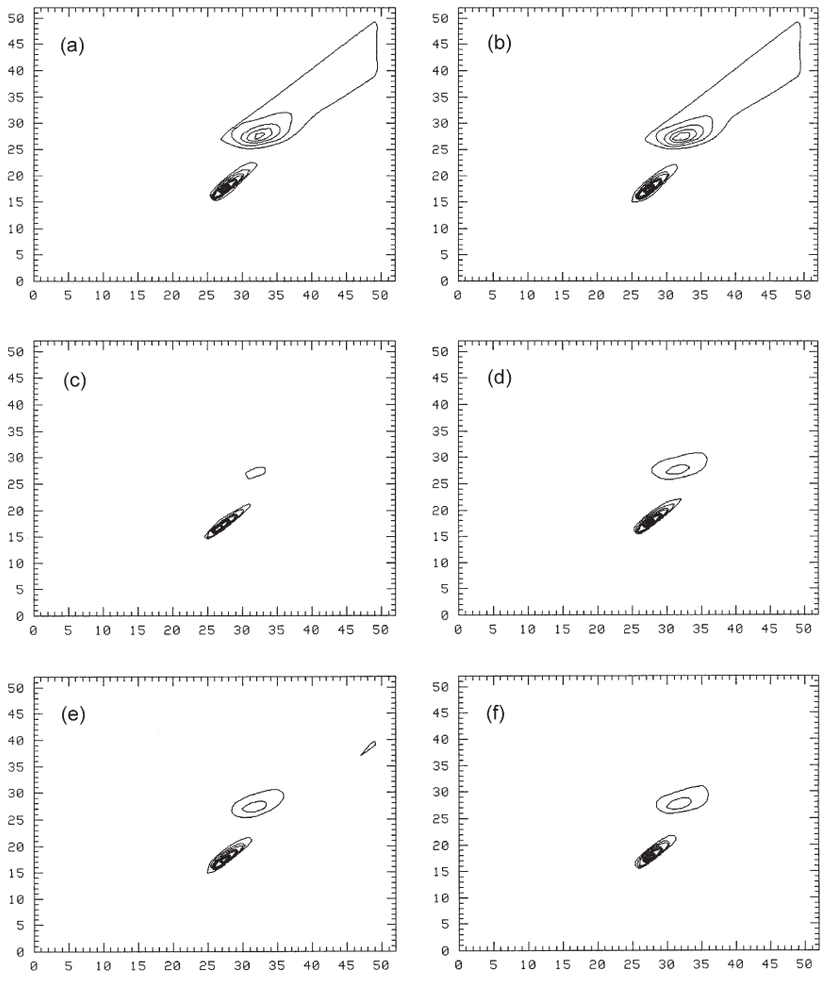

FIGURE 2 Contour map of the g_{OHO} function for the studied models. The internal OH distance is fixed. The abscissa shows the OO distance and the ordinate shows the external OH distance. Other properties are identical of that of the previous maps. (a) SPC; (b) SPC/E; (c) MSPC/E; (d) TIP4P; (e) TIP5P; (f) PPC.

we only calculated the overlap integrals O and O' for the g_{OOO} and g_{HHH} functions, which are given in Tables IV and V for the six water models.

The overlaps between the different g_{OOO} functions might seem quite large. Most of the values, especially those for the integral O calculated by Eq. (2), are close to 1. However, we should not forget that these models describe exactly the same liquid. Although we studied only a limited neighborhood of water molecules, the overwhelming part of the bins still contain values close to 1. The largest overlap was found between the SPC/E and TIP4P models, which are interesting because they belong to different families of interactions. It seems that the oxygen

TABLE IV Overlap integrals for g_{OOO} at 298 K

g_{OOO}	*SPC*	*SPC/E*	*MSPC/E*	*TIP4P*	*TIP5P*	*PPC*
SPC	1	0.934	0.877	0.955	0.913	0.938
SPC/E	0.986	1	0.931	0.970	0.958	0.958
MSPC/E	0.945	0.979	1	0.908	0.948	0.896
TIP4P	0.993	0.997	0.966	1	0.946	0.967
TIP5P	0.972	0.992	0.990	0.987	1	0.933
PPC	0.989	0.993	0.951	0.997	0.977	1

The upper half of the matrix contains the resulting values of the integral O' following Eq. (3), while the lower half contains the values of the integral O following Eq. (2).

TABLE V Overlap integrals for g_{HHH} at 298 K

g_{HHH}	*SPC*	*SPC/E*	*MSPC/E*	*TIP4P*	*TIP5P*	*PPC*
SPC	1	0.971	0.955	0.759	0.739	0.755
SPC/E	0.997	1	0.974	0.756	0.735	0.753
MSPC/E	0.983	0.985	1	0.758	0.735	0.748
TIP4P	0.396	0.395	0.402	1	0.949	0.960
TIP5P	0.393	0.391	0.398	0.988	1	0.959
PPC	0.396	0.394	0.401	0.994	0.990	1

The upper half of the matrix contains the resulting values of the integral O' following Eq. (3), while the lower half contains the values of the integral O following Eq. (2).

skeleton of this structure is very similar for these two models, despite the fact that their hydrogen bonding contains significant discrepancies. Expectedly, the SPC and MSPC/E pair showed the largest difference.

Note that, in contrast to Table IV, the overlap integrals for the g_{HHH} in Table V are less informative. The large differences between models of different families are due to the differences in their internal structures.

PARTIAL THREE-PARTICLE ENTROPY CONTRIBUTIONS

The entropy of a many body system can be calculated using the expansion of the correlation functions. The contributions can be assigned to the highest rank correlation function taking part in the integration. The convergence of the method by the rank of the correlation functions is limited, especially for molecular systems, but it can be used to quantify the order or disorder present at the given level of correlations [32–35]. Since the two-particle correlation functions of the different water models are visually obvious, we looked for significant differences in their three-body correlation functions. By integrating these correlation functions we can quantify the order or disorder present in these water model structures at the level of three-particle correlations.

The size of our model systems was too small to reach the asymptotic region of the distance-dependent three-body entropy contribution. There was little point in performing simulations for larger system because the presence of intra-molecular peaks would have destroyed the convergence anyhow. However, the running integration of the local entropy ensures that the value of the three-particle entropy characterizes the disorder within a sphere of radius shown at the abscissa.

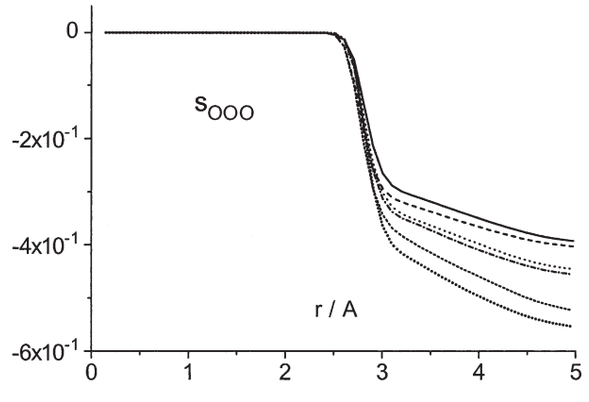

FIGURE 3 The running sum of the three-particle entropy function for the g_{OOO} function. (SOC: solid line; MSPC/E: dashed line; TIP4P: dotted line; SPC/E: dashed–dotted line; TIP5P: short dashed line; PPC: short dotted line. This is the order of the lines at the end of the graph from the top to the bottom).

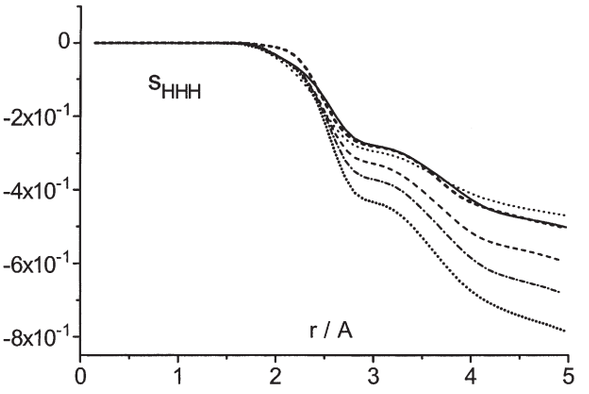

FIGURE 4 The running sum of the three-particle entropy function for the g_{HHH} function. (SPC: solid line; MSPC/E: dashed line; TIP4P: dotted line; SPC/E: dashed–dotted line; TIP5P: short dashed line; PPC: short dotted line. The line symbols are identical with that of the previous figure).

In Figs. 3 and 4, we show the first parts of these integrals for the g_{OOO} and the g_{HHH} partials. Although these functions obviously have not reached their asymptotic regions yet, the behavior of the curves yields an additional way to compare the local structures of the models. Differences in the cores of the models are small, i.e. hardly noticeable as shown in Fig. 3. However, in Fig. 4 the internal structures start the decline of the entropy differently. Being integrals, these curves are unable to show structural similarities between the models. But they are excellent probes for quantifying the relative order or disorder of a structure. In this respect, the SPC model creates the most disordered, while the PPC model gives the most ordered water structure among the studied models.

CONCLUSIONS

To summarize our findings we make contact with the recent work of Sorenson *et al.* [11,12] for two important reasons: they involve similar classical water models and, both makes the oxygen–oxygen correlation the center of the data processing. Sorenson *et al.* [11,12] claimed to provide the most accurate function of $g_{OO}(r)$ and, therefore, they used it as a reference to qualify classical models of water. Their comparison of $g_{OO}(r)$ to several earlier experimental results shows similar discrepancies to the uncertainties observed in the structure of different simulated models. This comes as no surprise in that the first and most important requirement in the development of effective pair-potentials is a good fit to the contemporary experimental function accepted as the best. We emphasize this point merely to warn against rushing

to an ultimate conclusion with respect to the quality of the models.

Our results point at the SPC model as the most disordered one. This is not in contradiction with Sorenson *et al.* [11,12] who claim that this model is too disordered. They also found that the similarity of TIP4P and SPC/E to the measured $g_{OO}(r)$ is roughly the same, and not too bad representation of the actual structure. That results agrees with our finding about the similarity of these two models, although we found a less-structured hydrogen bonding in the case of SPC/E. We also found that the PPC model predicted the most ordered structure out of the six potential models studied. This feature translates into a higher than the measured first peak in the studies of Sorenson *et al.* [11,12]. Finally, our study indicates that the MSPC/E structure exhibits the largest departure from the rest, especially from that of the SPC model. Unfortunately, this model was not analyzed by Sorenson *et al.* [11,12].

While the results discussed above seem to be a quantitative confirmation of the collective experience and wisdom of the area, the maps of the hydrogen bonding reveal remarkable behavior. While the SPC/E model gives a reasonably good structure, the map of its hydrogen bonding distribution is hardly different from that of the SPC model, which is much more disordered and considered to be a substantially poorer descriptor of the structure of ambient water. At the level of pair correlations the difference between the TIP4P and SPC/E is negligible, yet their higher order structure in terms of their hydrogen bonding is significantly different. It seems that hydrogen bonding is more sensitive to the molecular properties of the model than the overall structure of the system. Since the actual properties of liquid water can be closer to one of these models than the other, precise and comprehensive simulations are needed to decide which is the classical model to be refined.

An interesting situation involves the TIP5P water model, for which Sorenson *et al.* [11,12] found the best fit to their diffraction results. According to our analysis TIP5P is the second most structured model, although its structure is quite different from that of TIP4P and not particularly similar to that of PPC either. Obviously, because the simulation results used by Sorenson *et al.* [11,12] are the courtesy of several authors, their conclusions might be affected by the lack of uniformity in the system sizes, thermostating procedures, as well as the cutoff distance and handling of long range electrostatic interactions. For instance, it is well known that the smaller the system the more structured it appears. Moreover, the predicted microstructure and thermophysical behavior of a model are rather sensitive to the treatment of the long-range electrostatic interactions. In fact, the predicted behavior of the TIP5P model [25] changes significantly when the simple spherical cut-off is replaced by a more appropriate treatment of the long-range interactions [36]. Consequently, it might not be prudent to claim that, because the TIP5P gives a better representation of the water structure at ambient conditions, it will also be the best current water model available. Typically a non-polarizable water model that predicts a more structured fluid at ambient conditions also gives a rather poor representation of the structure at higher temperature or lower density, and consequently, it also predicts an inaccurate vapor–liquid phase envelope. In this regard, and according to the latest studies in Nezbeda's group at ICPF [36], TIP5P performs even worse than its predecessor TIP4P water model.

Acknowledgements

A. Baranyai gratefully acknowledges the support of OTKA grant T032481, AKP grant 2000-92,4 and the NATO Science Fellowship Program (1030/NATO/01). A.A. Chialvo acknowledges financial support from the Division of Chemical Sciences, Geosciences, and Biosciences, Office of Basic Energy Sciences under contract number DE-AC05-00OR22725 with Oak Ridge National laboratory, managed and operated by UT-Battelle, LLC. P.T. Cummings acknowledges financial support from the Division of Chemical Sciences, Geosciences, and Biosciences, Office of Basic Energy Sciences, of the U.S. Department of Energy.

References

[1] Narten, A.H. (1972) "Liquid water: atom pair correlation functions from neutron and X-ray diffraction", *Journal of Chemical Physics* **56**, 5681–5687.
[2] Narten, A.H., Thiessen, W.E. and Blum, L. (1982) "Atom pair distribution functions of liquid water at 25°C from neutron diffraction", *Science* **217**, 1033–1034.
[3] Soper, A.K. and Phillips, M.G. (1986) "A new determination of the structure of water at 25°C", *Chemical Physics* **107**, 47–60.
[4] Chialvo, A.A., Cummings, P.T., Simonson, J.M., Mesmer, R.E. and Cochran, H.D. (1998) "The interplay between molecular simulation and neutron scattering in developing new insights into the structure of water", *Industrial and Engineering Chemistry Research* **37**, 3021–3025.
[5] Beveridge, D.L., Mezei, M., Mehrotra, P.K., Marchese, F.T., Ravi-Shanker, G., Vasu, T. and Swaminathan, S. (1983) "Monte Carlo simulation studies of the equilibrium properties and structure of liquid water", In: Haile, J.M. and Mansoori, G.A., eds, *Molecular-Based Study of Fluids* (American Chemical Society, Washington, DC) **Vol. 204**, pp 298–351.
[6] Chialvo, A.A. and Cummings, P.T. (1999) "Molecular-based modeling of water and aqueous solutions at supercritical conditions", In: Rice, S.A., ed, *Advances in Chemical Physics* (Wiley, New York) **Vol. 109**, pp 115–205.
[7] Laasonen, K., Sprik, M., Parrinello, M. and Car, R. (1993) "*Ab initio* liquid water", *Journal of Chemical Physics* **99**, 9080–9089.
[8] Silvestrelli, P.L. and Parrinello, M. (1999) "Structural, electronic, and bonding properties of liquid water from first principles", *Journal of Chemical Physics* **111**, 3572–3580.

[9] Boero, M., Terakura, K., Ikeshoji, T., Liew, C.C. and Parrinello, M. (2001) "Water at supercritical conditions: a First Principles Study", *Journal of Chemical Physics* **115**, 2219–2227.
[10] Löffler, G., Schreiber, H. and Steinhauser, O. (1994) "Computer simulation as a tool to analyze neutron scattering experiments: water at supercritical temperatures", *Berichte der Bunsen-Gesellschaft fuer Physikalische Chemie* **98**, 1575–1578.
[11] Hura, G., Sorenson, J.M., Glaeser, R.M. and Head-Gordon, T. (2000) "A high-quality X-ray scattering experiment on liquid water at ambient conditions", *Journal of Chemical Physics* **113**, 9140–9148.
[12] Sorenson, J.M., Hura, G., Glaeser, R.M. and Head-Gordon, T. (2000) "What can X-ray scattering tell us about the radial distribution functions of water?", *Journal of Chemical Physics* **113**, 9149–9161.
[13] Kalinichev, A.G. (2001) "Molecular simulations of liquid and supercritical water: thermodynamics, structure, and hydrogen bonding", *Reviews in Mineralogy and Geochemistry* **42**, 83–129.
[14] Keutsch, F.N. and Saykally, R.J. (2001) "Water clusters: untangling the mysteries of the liquid, one molecule at a time", *Proceedings of the National Academy of Sciences of the United States of America* **98**, 10533–10540.
[15] George, W.O., Jones, B.F. and Lewis, R. (2001) "Water and its homologues: a comparison of hydrogen-bonding phenomena", *Philosophical Transactions of the Royal Society of London Series A—Mathematical Physical and Engineering Sciences* **359**, 1611–1629.
[16] Soper, A.K. (1994) "Orientational correlation function for molecular liquids: the case of liquid water", *Journal of Chemical Physics* **101**, 6888–6901.
[17] Svishchev, I.M. and Zassetsky, A.Y. (2000) "Three-dimensional picture of dynamical structure in liquid water", *Journal of Chemical Physics* **113**, 1367–1372.
[18] Pálinkás, G., Bopp, P., Jancsó, G. and Heinzinger, K.Z. (1984) "The effect of pressure on the hydrogen-bond structure of liquid water", *Zeitschrift fuer Naturforschung* **A39**, 179–185.
[19] Berendsen, H.J.C., Postma, J.P.M., van Gunsteren, W.F. and Hermans, J. (1981) "Interaction models for water in relation to protein hydration", In: Pullman, B., ed, *Intermolecular Forces: Proceedings of the Fourteenth Jerusalem Symposium on Quantum Chemistry and Biochemistry* (Reidel, Dordrecht), pp 331–342.
[20] De Pablo, J.J., Prausnitz, J.M., Strauch, H.J. and Cummings, P.T. (1991) "Molecular simulation of water along the liquid–vapor coexistence curve from 25°C to the critical point", *Journal of Chemical Physics* **93**, 7355–7359.
[21] Berendsen, H.J.C., Grigera, J.R. and Straatsma, T.P. (1987) "The missing term in effective pair potentials", *Journal of Physical Chemistry* **91**, 6269–6271.
[22] Boulougouris, G.C., Economou, I.G. and Theodorou, D.N. (1998) "Engineering a molecular model for water phase equilibrium over a wide temperature range", *Journal of Physical Chemistry B* **102**, 1029–1035.
[23] Guissani, Y. and Guillot, B.J. (1993) "A computer simulation study of the liquid–vapor coexistence curve of water", *Journal of Chemical Physics* **98**, 8221–8235.
[24] Jorgensen, W.L., Chandrasekhar, J., Madura, J.D., Impey, R.W. and Klein, M.L. (1983) "Comparison of simple potential functions for simulating liquid water", *Journal of Chemical Physics* **79**, 926–935.
[25] Mahoney, M.W. and Jorgensen, W.L. (2000) "A five-site model for liquid water and the reproduction of the density anomaly by rigid, nonpolarizable potential functions", *Journal of Chemical Physics* **112**, 8910–8922.
[26] Kusalik, P.G. and Svishchev, I.M. (1994) "The spatial structure in liquid water", *Science* **265**, 1219–1221.
[27] Hayward, T.M. and Svishchev, I.M. (2001) "Equations of state and phase coexistence properties for simulated water", *Fluid Phase Equilibria* **182**, 65–73.
[28] Nosé, S. (1984) "A unified formulation of the constant temperature molecular dynamics methods", *Journal of Chemical Physics* **81**, 511–519.
[29] Gear, C.W. (1996) *The Numerical Integration of Ordinary Differential Equations of Various Orders* (Argonne National Laboratory, Chicago).
[30] Evans, D.J. and Murad, S. (1977) "Singularity free algorithm for molecular dynamics simulation of rigid polyatomics", *Molecular Physics* **34**, 327–331.
[31] Neumann, M. (1983) "Dipole moment fluctuation formulas in computer simulations of polar systems", *Molecular Physics* **50**, 841–858.
[32] Baranyai, A. and Evans, D.J. (1989) "Direct entropy calculations from computer simulation of liquids", *Physical Review A* **40**, 3817–3822.
[33] Baranyai, A. and Evans, D.J. (1990) "3-Particle contribution to the configurational entropy of simple fluids", *Physical Review A* **42**, 849–857.
[34] Baranyai, A. and Evans, D.J. (1991) "On the entropy of the hard-sphere fluid", *Zeitschrift fuer Naturforschung A* **46**, 27–31.
[35] Borzsak, I. and Baranyai, A. (1992) "On the convergence of green entropy expansion", *Chemical Physics* **165**, 227–230.
[36] Lisal, M., Kolafa, J. and Nezbeda, I. (2002). Manuscript in preparation.